Materials Chemistry and Physics 236 (2019) 121812

Contents lists available at ScienceDirect

Materials Chemistry and Physics

journal homepage: www.elsevier.com/locate/matchemphys

Electronic polarizability and third-order nonlinearity of Nd^{3+} doped borotellurite glass for potential optical fiber

M.N. Azlan [a,*], M.K. Halimah [b], A.B. Suriani [a], Y. Azlina [a], R. El-Mallawany [c]

[a] Physics department, Faculty of Science and Mathematics, Universiti Pendidikan Sultan Idris, 35900, Tanjung Malim, Perak, Malaysia
[b] Physics department, Faculty of Science, Universiti Putra Malaysia, 43400, Serdang, Selangor, Malaysia
[c] Physics Department, Faculty of Science, Menoufia University, Egypt

HIGHLIGHTS

- The linear optical band gap and refractive index of the glass samples.
- The calculated optical parameters of electronic polarizability.
- The optical basicity and metallization criterion.
- The nonlinear optical properties and third order nonlinearity.

ARTICLE INFO

Keywords:
Glass
Borotellurite
Electronic polarizability
Optical basicity
Third-order nonlinearity

ABSTRACT

The glass series with composition of $\{[(TeO_2)_{0.70}\ (B_2O_3)_{0.30}]_{0.7}\ (ZnO)_{0.3}\}_{1-y}\ (Nd_2O_3)_y$ where, y = 0.005, 0.01, 0.02, 0.03, 0.04 and 0.05; was fabricated via melt-quenched technique. The third-order optical nonlinearity was observed by using Z-scan technique. Polarizability and third-order nonlinearity of borotellurite glass doped with neodymium (Nd^{3+}) will be reported. This work presents the effect of neodymium ions on the linear and nonlinear optical performance of borotellurite glass for potential photonics applications. The structure and optical performance of the resulting transparent neodymium doped borotellurite glass are characterized. The reduction of optical band gap energy, E_g is observed which shows the alteration of tellurite structure by the Nd^{3+}. The values of electronic polarizability are enhanced with an increase of Nd^{3+} ions. The enhancement of electronic polarizability provides an excellent medium for nonlinear optical applications. The optical basicity of the investigated materials shows non-linear trend along with Nd^{3+} ions concentration. The Z-scan data for third-order optical nonlinearities suggest that the glass materials are excellent to be used as a medium in nonlinear optical fiber. Therefore, the investigated glass materials may provide a good material for photonic applications.

1. Introduction

Tellurite glasses have an interesting physical properties when compared to borate or germanate or silicate or phosphate glasses [1–7]. The incorporation of borate oxide in tellurite glasses are the most stable glass and had been widely used due to their attractive characteristics which have potential used for specific applications [8–10]. The glass materials doped with various elements of rare-earth oxides have been extensively studied, mainly due to their important medium in laser glass, optical fibre and mode lock fibre laser [11]. Erbium doped fibre amplifier (EDFA) is one of the common applications in optical telecommunications. Furthermore, the silicate oxide, SiO_2 is largely used as a host materials for commercial optical telecommunications. However, silicate glass has high melting temperature and high absorption loss which degrades the capability of optical fiber [12]. Phosphate glass had been widely used in lasing materials and one of the examples is the commercial neodymium doped phosphate laser glass. The phosphate glass has high hygroscopic properties which leads to the corrosion and unstable in air [13]. This features give high disadvantage to the laser glass. The replacement of the current glass materials with the new materials is crucial especially to increase the optical performance and stability. The extensive research on tellurite glass shows that the TeO_2 has received high interest among the researchers due to its low melting temperature, low hygroscopic and low loss to replace the current silicate

* Corresponding author.
E-mail address: azlanmn@fsmt.upsi.edu.my (M.N. Azlan).

https://doi.org/10.1016/j.matchemphys.2019.121812
Received 7 May 2019; Received in revised form 30 June 2019; Accepted 2 July 2019
Available online 3 July 2019

and phosphate glasses [14]. The importance of tellurite glass to be used as a laser emission is of interest. In the development of tellurite glass as a laser glass, **Bell *et al.*** conducted a research on neodymium doped zinc-tellurite glass for high emission of laser glass [15]. Based on the reports, the presence of neodymium oxide in tellurite glass provides a low laser threshold of 8 mW and low internal losses. Subsequently, the studied tellurite glass was shown to have high lifetime of emission in the range of 210 μs and large stimulated emission cross section of 3.1×10^{-20} cm^2. Such features suggest tellurite laser glass as an efficient photonic devices. The excellent optical efficiency of the Nd^{3+}-tellurite glass had raised the number of research to develop an excellent laser application. **Wei *et al.*** stated that Nd^{3+} possesses outstanding properties such as several excited levels that are useful for optical pumping and longer fluorescence lifetimes [16]. It was also stated that 1.06 μm emission can be produced by using commercial 808 nm laser diode. These features indicate that Nd^{3+} doped glasses are commercially necessary which increases the study on optical efficiency of Nd^{3+} in various glass network. Hence, the study of Nd^{3+} doped borotellurite glass may provide high possibility of developing new materials for photonic applications.

In recent research, there are some studies on the effect of neodymium on optical band gap and 1.06 μm emission band of tellurite glass, but there are limited study on the polarizability and third order optical nonlinearity of neodymium doped borotellurite glass [17]. Hence, the present research is focused on the development of neodymium doped borotellurite glass for optical fibre and lasing materials. This work consists of the characterization of Fermi energy, optical band gap, electronic polarizability and third order optical nonlinearity.

2. Experimental

The glass series with composition of $\{[(TeO_2)_{0.70}\ (B_2O_3)_{0.30}]_{0.7}\ (ZnO)_{0.3}\}_{1-y}\ (Nd_2O_3)_y$ where, y = 0.005, 0.01, 0.02, 0.03, 0.04 and 0.05; was fabricated via melt-quenched technique. The chemical compositions (in wt%) used for the preparation of the titled glass system are shown in Table 1. Each of the raw materials was weighed according to the chemical composition. The raw materials were mixed in a platinum crucible thoroughly. The compound in a platinum crucible was transferred in a furnace with heating temperature of 400 °C at 1 h for annealing process. The mixture was transferred to a second furnace with heating temperature of 900 °C at 2 h for melting process. The molten of the mixture was formed during the melting process. The molten was quenched in a cylindrical stainless steel would that had been pre-heated at 400 °C for 1 h. The molten in the mold was transferred to a furnace with heating temperature of 400 °C at 1 h to enhance its mechanical strength. The furnace was turned off and the sample was allowed to cool down to room temperature. The glass sample was cut in a pallet form. The XRD was carried out by using X'pert pro pan analytical. The refractive index of the glass system was measured by using EL X–02C high precision Ellipsometer. The absorption spectra of the glass system were carried out by using Shimadzu UV–Vis spectrophotometer. The third-order optical nonlinearity was observed by using Z-scan technique.

Table 1
Glass composition $\{[(TeO_2)_{0.70}\ (B_2O_3)_{0.30}]_{0.7}\ (ZnO)_{0.3}\}_{1-y}\ (Nd_2O_3)_y$ where, y = 0.005, 0.01, 0.02, 0.03, 0.04 and 0.05.

Sample	Glass composition	Percentage of Nd^{3+}
1	$\{[(TeO_2)_{0.70}\ (B_2O_3)_{0.30}]_{0.7}\ (ZnO)_{0.3}\}_{0.995}$ $(Nd_2O_3)_{0.005}$	0.5%
2	$\{[(TeO_2)_{0.70}\ (B_2O_3)_{0.30}]_{0.7}\ (ZnO)_{0.3}\}_{0.99}$ $(Nd_2O_3)_{0.01}$	1%
3	$\{[(TeO_2)_{0.70}\ (B_2O_3)_{0.30}]_{0.7}\ (ZnO)_{0.3}\}_{0.98}$ $(Nd_2O_3)_{0.02}$	2%
4	$\{[(TeO_2)_{0.70}\ (B_2O_3)_{0.30}]_{0.7}\ (ZnO)_{0.3}\}_{0.97}$ $(Nd_2O_3)_{0.03}$	3%
5	$\{[(TeO_2)_{0.70}\ (B_2O_3)_{0.30}]_{0.7}\ (ZnO)_{0.3}\}_{0.96}$ $(Nd_2O_3)_{0.04}$	4%
6	$\{[(TeO_2)_{0.70}\ (B_2O_3)_{0.30}]_{0.7}\ (ZnO)_{0.3}\}_{0.95}$ $(Nd_2O_3)_{0.05}$	5%

3. Results and discussion

3.1. X-Ray Diffraction analysis and FTIR analysis

Fig. 1 revealed the XRD patterns of Nd^{3+} doped borotellurite glass in the form $\{[(TeO_2)_{0.70}\ (B_2O_3)_{0.30}]_{0.7}\ (ZnO)_{0.3}\}_{1-y}\ (Nd_2O_3)_y$ where, y = 0.005, 0.01, 0.02, 0.03, 0.04 and 0.05. The observed broad hump at lower diffraction angle indicates the amorphous structural arrangement in the glass system. It is proved that the glass system is fully amorphous.

The assignments of elements of the studied glass system are obtained from the FTIR analysis. The FTIR spectra was depicted in Fig. 2, meanwhile, Table 2 revealed the details of the assignments for the glass system. The tellurite oxide consists of TeO_2 structural arrangement before the glass formation [18]. The breaking linkage of TeO_2 is done by the inclusion of oxide modifiers after the glass formation by converting the TeO_4 bridging oxygen to TeO_3 non-bridging oxygen [19]. The first absorption band is located in the range of 640 cm^{-1} to 649 cm^{-1} which indicates the high concentration of TeO_3 structural unit. Meanwhile, the absorption band at 1220 cm^{-1} to 1367 cm^{-1} is assigned to the BO_3-nonbridging structural unit. The BO_3 structural units consist of several stretching vibration groups which are metaborate, pyborate and orthoborate groups [20]. The intense absorption band of BO_3 units indicates the high number of non-bridging oxygen in the glass system. The ZnO structural assignments are unable to be located due to the breaking of ZnO lattice structure after the glass formation [14]. Meanwhile, the structural assignment for Nd^{3+} is not presence which is due to the low concentration of Nd^{3+}.

3.2. Optical absorption spectra, extinction coefficient and fermi energy

The absorption spectra in the visible region of the studied glass are revealed in Fig. 3. The sharp peaks indicating several energy transitions are revealed in the figure. This trend is due to the effect of 4f-4f orbital in the glass system. The magnetic dipole and forced electric dipole of Nd^{3+} are the main contributors to the observed sharp intensities in the absorption spectra. The spectral lines which associate with f-f transition are located from the ground state $^4I_{9/2}$ to the excited states $^2P_{3/2}$, $^4G_{7/2}$, $^4G_{5/2}$, $^4F_{9/2}$, $^4F_{7/2}$, $^4F_{5/2}$ and $^4F_{3/2}$. It is noted that the intensity of the energy transitions is enhanced with an increase of Nd^{3+}. According to Derr, 1980, the extinction coefficient can be described as a rate of the light transmission due to scattering and absorption of a particular medium [21]. The extinction coefficient spectra of a glass can be obtained from Fermi-Dirac relation, meanwhile the Fermi energy is determined by using least-square fitting of Fermi-Dirac relation [22]. Fig. 4 shows the extinction coefficient spectra of the studied glass. The trend of extinction coefficient spectra of the glass system shows a steep increase near ultraviolet (UV) region which indicates a strong value in the UV region. Meanwhile, the extinction coefficient is found to decrease with an increase of Nd^{3+}. The Fermi energy of the glass system can be calculated by using the least square fitting of Fermi-Dirac distribution function. Table 3 shows the tabulated data of Fermi energy of the glass system. It can be seen from the table that the value of Fermi energy, E_F reduces with an increase of Nd^{3+}. The reduction of Fermi energy, E_F indicates the improvement of semiconducting properties. Moreover, the value of Fermi energy, E_F is found lower than the value of thermal energy at room temperature ($k_BT \sim 25$ meV). Consequently, the glass system shows a tendency towards semiconducting behavior.

3.3. Refractive index, optical band gap and urbach energy

Fig. 5 shows the trend of refractive index along with Nd^{3+} content. It is shown that the refractive index, n is enhanced with an increase of

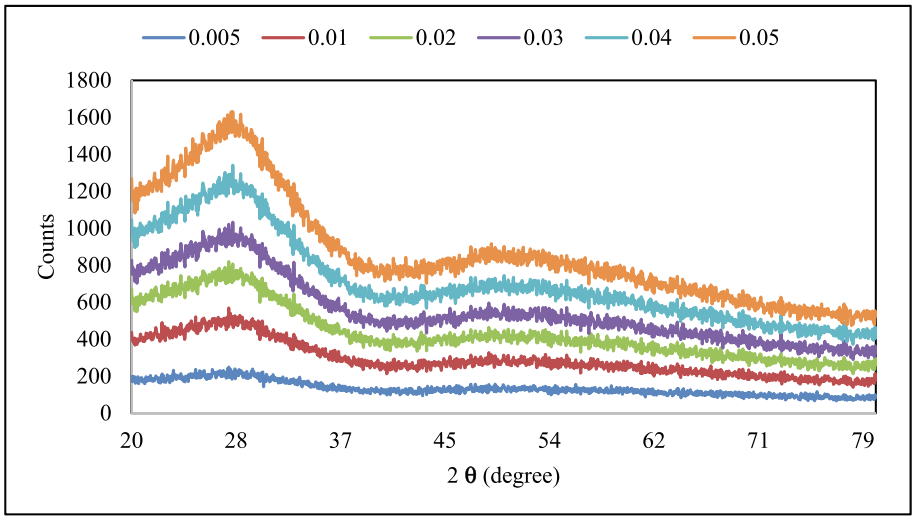

Fig. 1. X-Ray Diffraction spectra.

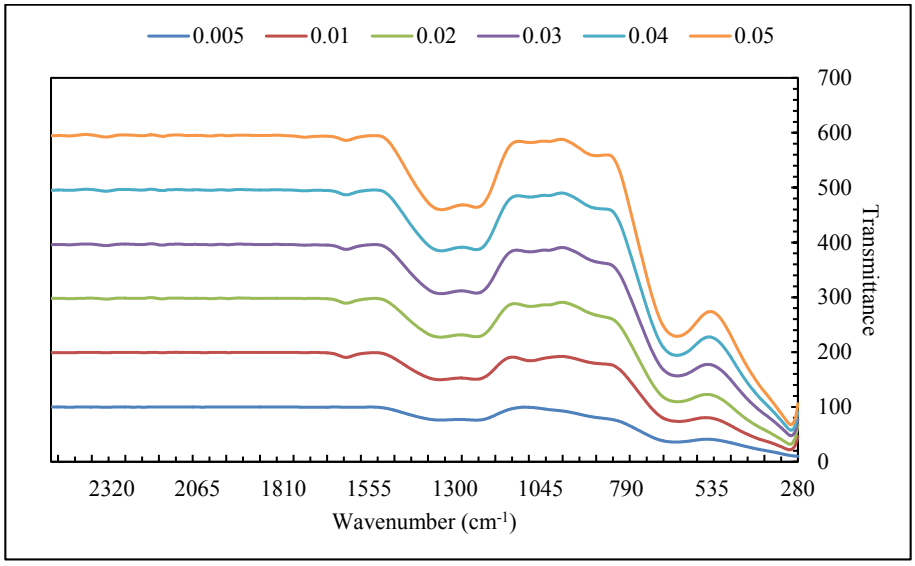

Fig. 2. Fourier Transform Infrared spectra.

Table 2
Transmission assignments for Nd^{3+} doped borotellurite glasses $\{[(TeO_2)_{0.70}(B_2O_3)_{0.30}]_{0.7}(ZnO)_{0.3}\}_{1-y}(Nd_2O_3)_y$ where, y = 0.005, 0.01, 0.02, 0.03, 0.04 and 0.05

No	0.005	0.01	0.02	0.03	0.04	0.05	Assignments
1	1347	1338	1362	1357	1377	1367	Trigonal B–O bond stretching vibrations in isolated trigonal BO_3 units
2	1220	1210	1221	1221	1225	1222	Trigonal B–O bond stretching vibrations of BO_3 units from boroxyl groups
3	649	644	645	635	649	640	TeO_3 stretching vibrations

Nd^{3+} from 1.760 to 1.863. The enhancement of refractive index can be explained by the role of Nd^{3+} to alter the structural properties of borotellurite glass system. The addition of Nd^{3+} leads to the modification of the glass network by converting the TeO_4 tetrahedral to TeO_3 triangular [23]. The conversion of tellurite oxide structure leads to the creation of non-bridging oxigen which increase the polarizability of the glass network. The high polarizability of lone pair in non-bridging oxygen results to an increase of refractive index. The creation of non-bridging oxygen leads to the formation of ionic bonds which increase the number of refractive index. Fig. 6 shows the Tauc's plot of $(\alpha h\nu)^{1/2}$ for indirect allowed transitions of the glass system [24]. The values of optical band gap, E_{opt} has been estimated by extrapolating the absorption coefficient curves and the obtained results are shown in Fig. 7 and listed in Table 4. Fig. 7 shows the reduction of optical band gap energy with an increase of Nd^{3+}. The shifts of valence and conduction band leads to the change in optical band gap energy. The reduction in optical band gap energy indicates that the forbidden gap is decreased. Moreover, the structural change in the glass network leads to the shifts of forbidden gap which affect the optical band gap energy [14]. The role of non-bridging oxygen contributes to the increasing number of free electrons which are less tightly bound to the nuclear charge. The free electrons have high ability to excite from the valence band to the conduction band which in turn leads to the reduction of optical band gap energy. Furthermore, the inclusion of Nd^{3+} ions in the glass system increase the number of weaker bonds which reduce the number of optical band gap energy [25]. Moreover, the decline in optical band gap energy is caused

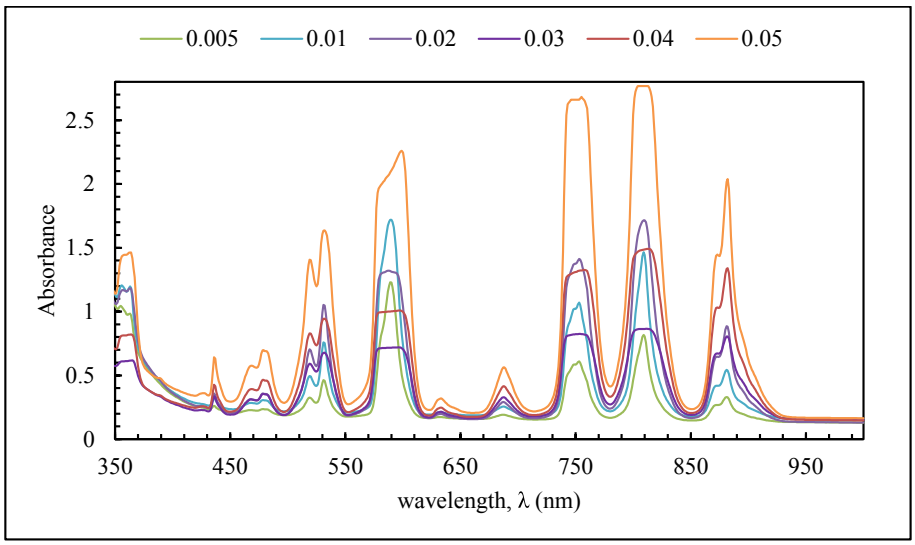

Fig. 3. UV–Visible absorption spectra.

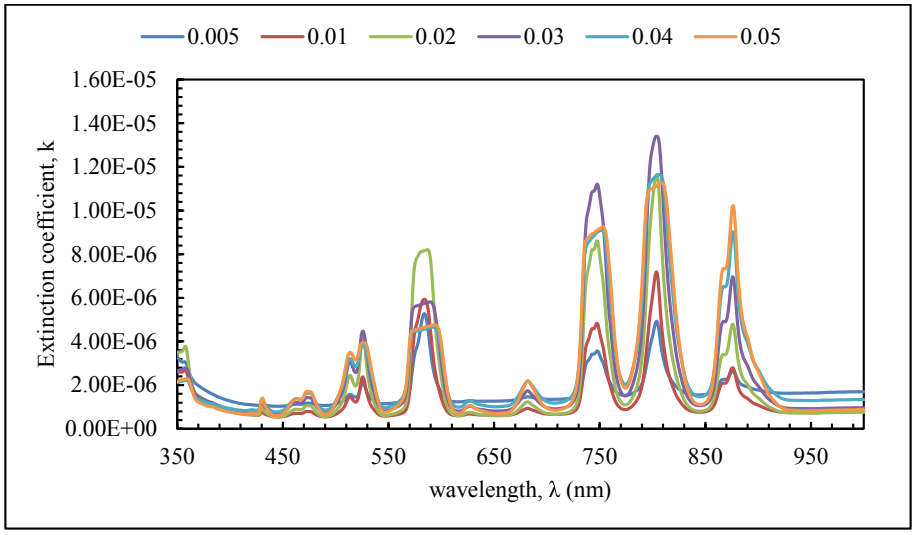

Fig. 4. Extinction coefficient versus wavelength.

Table 3
Fermi Energy of Nd^{3+} doped borotellurite glasses $\{[(TeO_2)_{0.70}(B_2O_3)_{0.30}]_{0.7}(ZnO)_{0.3}\}_{1-y}(Nd_2O_3)_y$ where, y = 0.005, 0.01, 0.02, 0.03, 0.04 and 0.05

Mol fraction	Fermi Energy, E_F (eV)
0.005	3.686
0.01	3.611
0.02	3.491
0.03	3.441
0.04	3.301
0.05	3.270

by the presence of TeO_3 non-bridging oxygen atoms, the high field strength of Nd^{3+} and high polarizing power of non-bridging oxygen. The information of rigidity in the glass matrix is explained by the value of Urbach energy. The values of Urbach energy of the glass system are tabulated in Table 4. The increasing trend of Urbach energy is revealed with an increase of Nd^{3+}. This trend may be contributed by the number of defects in the glass network. The increase of defects in the glass network leads to an increase of Urbach energy. Furthermore, the degree of disorderliness in the glass system can be analyzed by using the Urbach energy value. The increase of Urbach energy indicates that the glass structure tends to be more disorder and weaker with an increase of Nd^{3+}.

3.4. Electronic polarizability and oxide ion polarizability

The values of electronic polarizability and oxide ion polarizability were calculated by using Lorentz-Lorentz equation [26].

$$\alpha_m = \frac{3}{4\pi N_A} R_m \quad (1)$$

where N_A denotes the Avogadro's number in which correspond to the number of polarizable ions per mole. The values of electronic polarizability for Nd^{3+} doped borotellurite glasses calculated in this study are given in Table 5 and plotted in Fig. 8. The figure shows the compositional dependence of electronic polarizability. The increasing trend of electronic polarizability is displayed as the concentration of Nd^{3+} increases. The deformability of electron cloud is affected by the number of non-bridging oxygen exists in the glass system. Non-bridging oxygen consists of free electrons from the lone pair which are less tightly bound

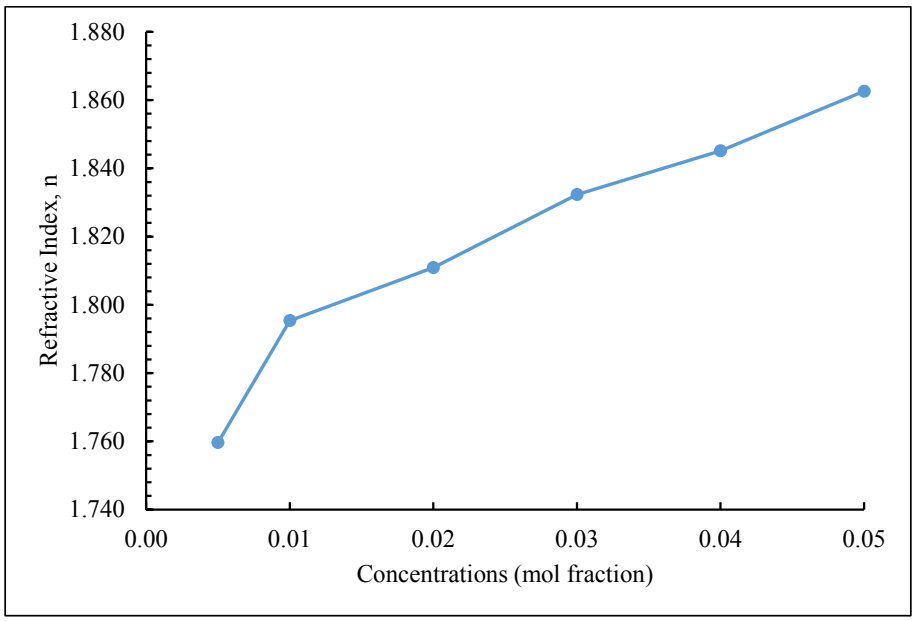

Fig. 5. Refractive index versus concentration of Nd^{3+}.

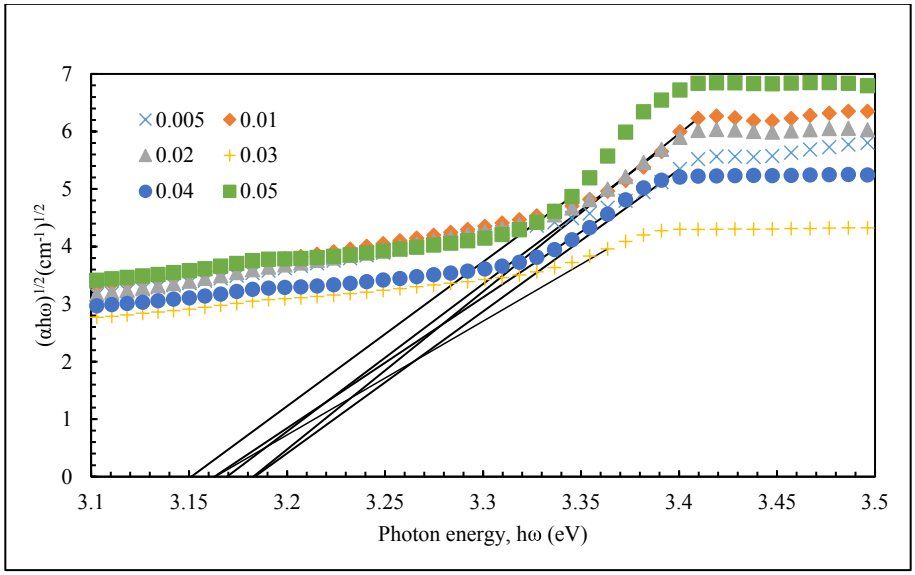

Fig. 6. $(\alpha\hbar\omega)^{1/2}$ versus photon energy $\hbar\omega$

to the nuclear charge. Consequently, the free electrons are easily polarized as the electrical field is penetrated through the medium [27]. The number of non-bridging oxygen ions is increased as the concentration of Nd^{3+} increases. The increment number of non-bridging oxygen leads to the raised number of free electrons in the glass system. Hence, the electronic polarizability is increased as the concentration of Nd^{3+} increases. The results of oxide ion polarizability of Nd^{3+} doped borotellurite glasses are listed in Table 5 and plotted in Fig. 8. The non-linear trend of oxide ion polarizability values is found in the glass series. The lowest value of oxide ion polarizability of Nd^{3+} doped borotellurite glasses is at 0.005 mol fraction. The values of oxide ion polarizability are found to increase up to 0.04 mol fraction. Previously, it has been suggested that the increasing number of refractive index leads to a rise of oxide ion polarizability [28]. This is due to the direct relationship of molar refraction with oxide ion polarizability [29]. Meanwhile, the value of oxide ion polarizability decreases at 0.05 mol fraction. This trend is due to the structural change in the glass matrix at 0.05 mol fraction of Nd^{3+}.

3.5. Optical basicity and metallization criterion

The value of optical basicity was calculated by using relation below [20].

$$\Lambda = X_1\Lambda_1 + X_2\Lambda_2 + \ldots\ldots + X_n\Lambda_n \quad (2)$$

Where $X_1, X_2, \ldots, X_n$ correspond to the equivalent fractions of oxides and $\Lambda_1, \Lambda_2, \ldots, \Lambda_n$ correspond to the optical basicity of oxides in the studied glass system. Meanwhile, the value of metallization criterion was obtained by using an equation as follows [20].

$$M = 1 - \frac{R_m}{V_m} \quad (3)$$

where R_m is molar refraction and V_m is molar volume. The obtained data

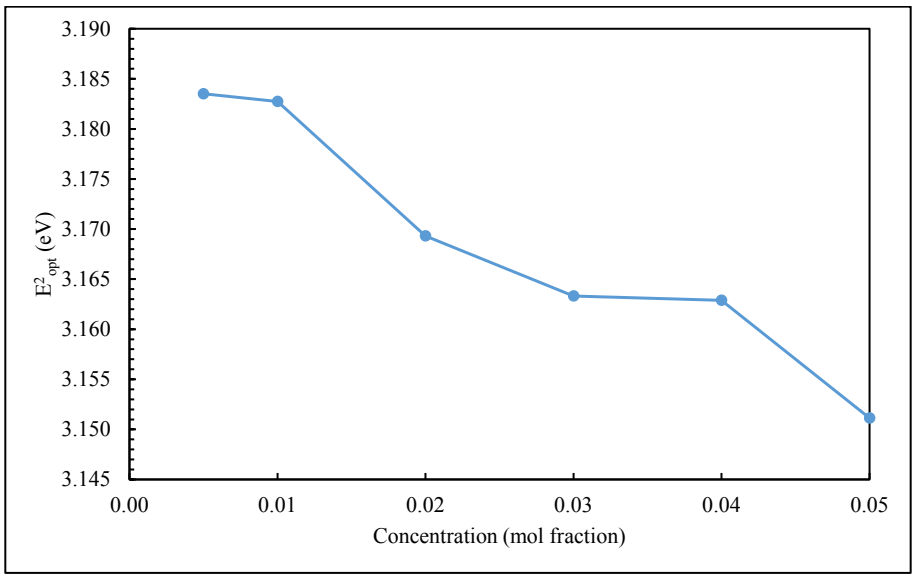

Fig. 7. Optical band gap energy.

Table 4
Optical band gap (E_{opt}) and Urbach energy (ΔE) of Nd^{3+} doped borotellurite glass system $\{[(TeO_2)_{0.70}\ (B_2O_3)_{0.30}]_{0.7}\ (ZnO)_{0.3}\}_{1-y}\ (Nd_2O_3)_y$ where, y = 0.005, 0.01, 0.02, 0.03, 0.04 and 0.05

Mol fraction	E_{opt} (eV)	Urbach energy, ΔE(eV)
0.005	3.331	0.316
0.01	3.323	0.316
0.02	3.320	0.317
0.03	3.311	0.319
0.04	3.310	0.318
0.05	3.307	0.320

Table 5
Electronic polarizability and oxide ion polarizability of Nd^{3+} doped borotellurite glasses $\{[(TeO_2)_{0.70}\ (B_2O_3)_{0.30}]_{0.7}\ (ZnO)_{0.3}\}_{1-y}\ (Nd_2O_3)_y$ where, y = 0.005, 0.01, 0.02, 0.03, 0.04 and 0.05

Mol fraction	Electronic Polarizability, α_m (Å)	Oxide ion polarizability, $\alpha_{o^{2-}}$ (Å)
0.005	5.265	2.279
0.01	5.452	2.352
0.02	5.567	2.363
0.03	5.698	2.382
0.04	5.795	2.384
0.05	5.843	2.361

of optical basicity for Nd^{3+} doped borotellurite glasses are tabulated in Table 6 and plotted in Fig. 9. The large value of optical basicity in the glass series revealed that the glass system is more basic. Oxide ions in the glass system act as a Lewis base which donate electrons to the surrounding cations. The high degree of donating ability of oxide ions influence strongly to the acid-base characteristic. Furthermore,it has been proposed that the optical basicity is related to the polarization state of oxide ions in the glass system [30]. Low polarizing cations in the glass system contributes to the strong donating ability of oxide ions to the surroundings cations. Based on the previous data of oxide ion polarizability, there is a good agreement with optical basicity.

The non-linear trend of optical basicity along with concentration are found in the glass system. The non-linear trend of optical basicity is caused by the structural change in the glass system. Besides that, the optical basicity values are found slightly increases with increasing concentration of Nd^{3+}. This trend can be explained by comparing the value of optical basicity of single element in the glass system. In

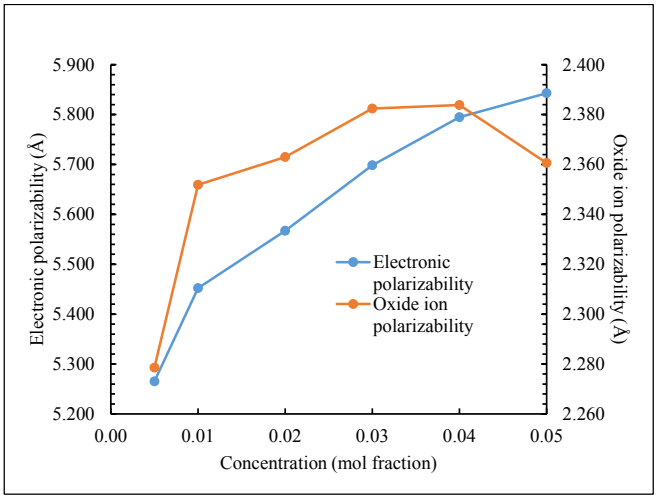

Fig. 8. Electronic polarizability and oxide ion polarizability.

Table 6
Optical basicity and metallization criterion of Nd^{3+} doped borotellurite glasses $\{[(TeO_2)_{0.70}\ (B_2O_3)_{0.30}]_{0.7}\ (ZnO)_{0.3}\}_{1-y}\ (Nd_2O_3)_y$ where, y = 0.005, 0.01, 0.02, 0.03, 0.04 and 0.05

Mol fraction	Optical basicity, Λ	Metallization criterion
0.005	1.401	0.589
0.01	1.400	0.574
0.02	1.399	0.568
0.03	1.397	0.560
0.04	1.396	0.555
0.05	1.173	0.549

conditions of glass former and modifier, former oxides should less basic compare with modifier oxides. The addition of modifier oxide to former oxide results the modification reaction to be the acid-base reaction in which the acidic region of former oxide is approached by modifier oxide ion in order of decreasing acidities [31]. The obtained values of metallization criterion of Nd^{3+} doped borotellurite glasses are tabulated in Table 6 and plotted in Fig. 9. The results show that the value of metallization criterion is decreased along with concentration. The decline in

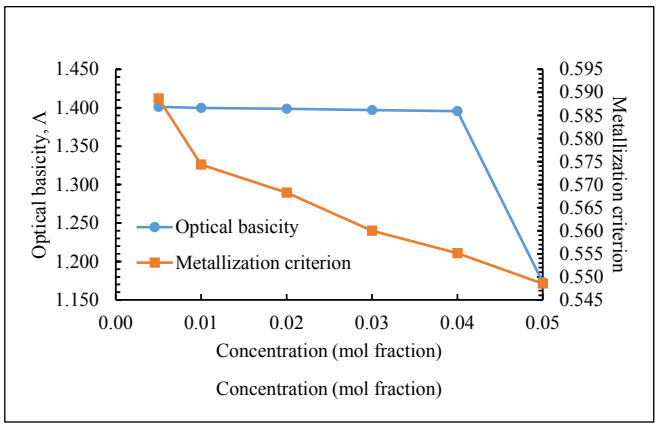

Fig. 9. Optical basicity and metallization criterion.

metallization criterion shows the metallizing of the glass samples which leads to tailing and shrinking of the band gap [32]. Metallization criterion depends on the band gap of the glass system. The decrement value of optical band gap indicates that the valence and conduction band are broadened. This effect will lead to the metallization of the glass system.

3.6. Non-linear refractive index

Factors that affect nonlinearity of refractive index are electronic polarizability, electrostriction, molecular orientation, photorefractive effect, and thermal effect [33]. Moreover, the nonlinear refractive index consists of third or higher order nonlinearity. The close aperture curves indicating the nonlinear refractive index of Nd^{3+} doped borotellurite glass are depicted in Fig. 10. The nonlinear refraction coefficient, η_0 (cm^2/W) of Nd^{3+} dopant obtained in the present work are listed in Table 7. It can be seen that the Z-scan curves exhibit peak-and-valley ration which corresponds to positive nonlinear refraction ($\eta_2 > 0$) and self-focusing behavior. The negative or positive sign of nonlinear refractive index correlate to self-defocusing and self-focusing are depended on sample properties. In the case of self-focusing, as the sample glass move closer to the focal area, the incident laser is diverged and leads to an increase in irradiance before it arrives at the focal point. As the sample arrives at the focal point, the incident laser is collimated and caused a decrease in irradiance [34]. It is observed that the distance of peak-to-valley is approximately 1.7 times of Rayleigh length from the laser source. Hence, it is confirmed that the nonlinear refractive index is caused by the third-order response.

It can be seen from Table 7 that the nonlinear refractive index coefficient for Nd^{3+} is in nonlinear variation along with dopants concentration. This variation might be due to the effect of dopants concentration. Moreover, the nonlinear refractive index for Nd^{3+} are in high value. The nonlinear refractive index is related to the value of the linear refractive index. Chen et al. [35] stated that a glass material which has a high refractive index possess high nonlinear refractive index. Previous data of linear refractive index reported that Nd^{3+} dopants have a high value of the linear refractive index. Hence, it corresponds to the high value of the nonlinear refractive index of Nd^{3+} dopants. The maximum point of nonlinear refractive index of Nd^{3+} are 0.04 and 0.01 mol fraction respectively. The increasing number of the nonlinear refractive index is highly related to the formation of $[TeO_3]^{2-}$ clusters in the glass matrix. The formation of TeO_3 clusters is proved from the previous FTIR spectra. The presence of lone pair in TeO_3 structural units leads to an increase in polarizability. Consequently, the increment of polarizability caused an increase in the nonlinear refractive index. The reduction in the nonlinear refractive index at a certain amount of Nd^{3+} is due to the effect of structural defects in the glass matrix.

3.7. Non-linear optical absorption

The nonlinear optical absorption is measured by using the open aperture mode from the Z-scan technique (S = 1). Moreover, the nonlinear absorption can be divided into two conditions: a. saturation absorption, b. reverse saturation absorption. The existence of valley curves at focus point (Z = 0) corresponds to saturation absorption, meanwhile the presence of a peak at focus point (Z = 0) is ascribed to reverse saturation absorption. The valley curves indicating nonlinear absorption of Nd^{3+} are shown in Fig. 11. It is confirmed that the nonlinear absorption is in saturation absorption. It is observed that the optical transmission is decreased towards the laser focus (z = 0) which ascribed to the occurrence of nonlinear absorption as the laser density decreased. The presence of valley curves proved the existence of two-photon absorption (2 PA) at a fix visible laser wavelength. The calculation of nonlinear optical absorption coefficient is made by fitting the curves using the equation below

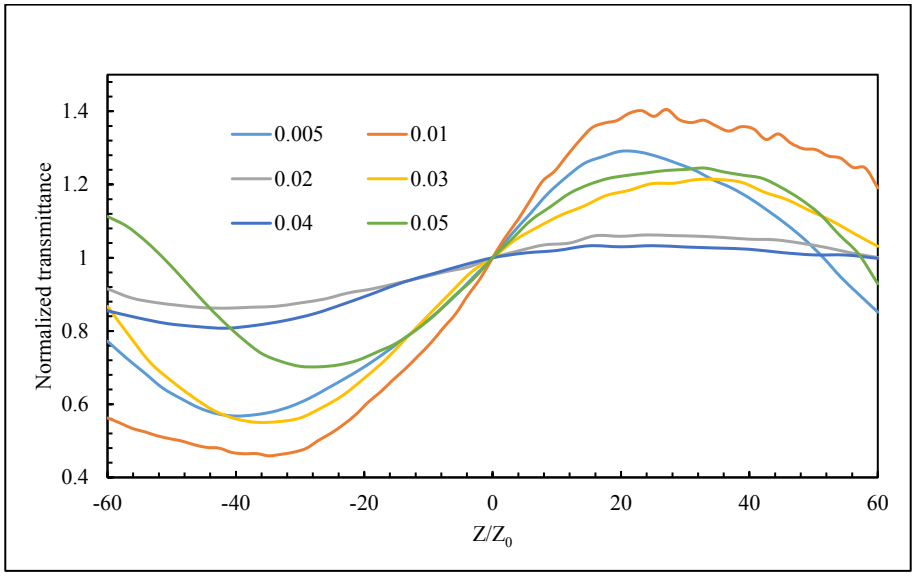

Fig. 10. Z-scan closed aperture curves.

Table 7
Nonlinear refractive index, η of Nd^{3+} doped borotellurite glasses $\{[(TeO_2)_{0.70}\ (B_2O_3)_{0.30}]_{0.7}\ (ZnO)_{0.3}\}_{1-y}\ (Nd_2O_3)_y$ where, y = 0.005, 0.01, 0.02, 0.03, 0.04 and 0.05

Mol fraction	Phase change, ΔØ	Linear absorption coefficient, α	Non-linear refractive index, η (x 10^{-12})	Nonlinear absorption, β (x 10^{-3})	Third order susceptibilities, χ (x 10^{-6})
0.005	0.11	13.62	2.35	1.52	5.06
0.01	0.06	12.72	1.29	2.95	10.2
0.02	0.10	9.95	2.20	1.42	4.99
0.03	0.04	4.69	1.00	1.86	6.71
0.04	0.18	7.02	4.15	7.49	27.3
0.05	0.03	15.93	0.633	4.84	18.0

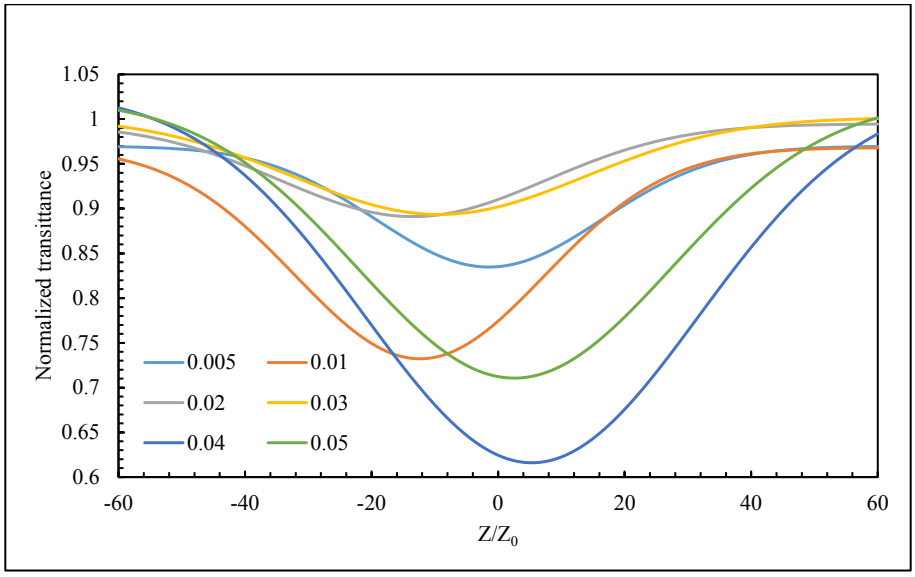

Fig. 11. Z-scan open aperture curves.

$$T(z) = \frac{\ln[1 + q_0(z)]}{q_0(z)} \quad (4)$$

The obtained value of nonlinear absorption coefficient is tabulated in Table 6. It can be seen that the nonlinear absorption coefficient exhibits nonlinear variations which are due to the effect of dopants concentration. The highest value of nonlinear absorption coefficient is at 0.04 mol fraction. The increment of nonlinear absorption coefficient can be attributed to the increasing number of non-bridging oxygen in the glass matrix. It has been stated that the valence electrons in non-bridging oxygen are less stable and weakly bound to the host materials [36]. Consequently, the valence electrons are easy to deform by the laser electromagnetic field which leads to an increase in nonlinear absorption coefficient. The FTIR studies also reported that the non-bridging oxygen is increased with increasing content of Nd^{3+}. Slightly decreases of nonlinear absorption coefficient are found in the glass system. This trend is attributed to the loss of a few fractions of photocarriers from the ground state [37]. Hence, when the incident laser intensity is greater than saturation intensity, the nonlinear absorption coefficient is decreased. The small value of nonlinear absorption coefficient indicates that the present glass sample is suitable for optical limiting devices.

The third order susceptibility of Nd^{3+} are calculated by applying η_2 and β values as shown in the following equation;

$$\left|X^{(3)}\right| = \left[\left(ReX^{(3)}\right)^2 + \left(ImX^{(3)}\right)^2\right]^{1/2} \quad (5)$$

Moreover, the third order susceptibility consists of real parts, Re (χ) and imaginary parts, Im (χ) which are obtained by using the nonlinear refractive index, η_2 and nonlinear absorption coefficient, β. The obtained data of third order susceptibility of the glass system are tabulated in Table 6. It is observed that the third order susceptibility of Nd^{3+} doped borotellurite glasses exhibit nonlinear variations. The third order nonlinearity is highly related to the structural properties of the glass network. Table 6 revealed that the highest susceptibility of Nd^{3+} doped borotellurite glass is at 0.05 mol fraction. The dependence of χ on the structure of the glass network indicates that the high intensity of [TeO_3] pyramidal in the glass network enhance the value of third order susceptibility. The formation of [TeO_3] pyramidal is proved from the previous data of FTIR. Moreover, the increase in nonlinearity of the glass system is associated with the higher ratio of oxygen-to-cation which consequently increase the polarizability of the glass system [38]. A slight decrease of third order susceptibilities of Nd^{3+} doped borotellurite glasses is due to the effect of dopants compositions [28]. Moreover, the decreasing variations of third order susceptibility can be due to the substitutions of higher polarizable compounds with lower polarizable compounds in the glass network.

4. Conclusion

The glass series was successfully prepared by using melt-quenching method. The effect of Nd3+ has been studied by:

- The values of electronic polarizability of borotellurite glasses are increased with increasing concentration of Nd3+ (5.265–5.843 Å)
- The obtained results of oxide ion polarizability of borotellurite glasses are found in nonlinear trend along with the concentration of Nd3+ (2.279–2.361 Å)
- The nonlinear trend of optical basicity is found in borotellurite glass system with increasing concentrations of Nd3+ (1.401–1.173)
- The decreasing value of metallization criterion was found in Nd3+ doped borotellurite glass (0.589–0.549)

- The non-linear trend of nonlinear refractive index and nonlinear optical absorption was found
- The decrease in third-order susceptibility is found which is due to the effect of Nd3+ by enhance the polarizability of the glass system.

Acknowledgement

This research was financially supported by Geran Penyelidikan Universiti (GPU), Sultan Idris Education University (Grant code: 2018-0139-103-01) and Skim Geran Penyelidikan Fundamental (FRGS) Fasa 1/2018 (Grant code: 2019-0006-102-02). The authors would like to thank the following institutions for equipment support: Faculty of Science and Mathematics, Universiti Pendidikan Sultan Idris and Faculty of Science,Universiti Putra Malaysia.

References

[1] R. El-Mallawany, M.I. Sayyed, M.G. Dong, Comparative shielding properties of some tellurite glasses: Part 2, J. Non-Cryst. Solids 474 (2017) 16–23.
[2] R. El-Mallawany, Specific heat capacity of semiconducting glasses: binary vanadium tellurite, Physica Status Solidi (A) Applied Research 177 (2) (2000) 439–444.
[3] R. El-Mallawany, A. Abd El-Moneim, Comparison between the elastic moduli of tellurite and phosphate glasses, Physica Status Solidi (A) Applied Research 166 (2) (1998) 829–834.
[4] M.M. Elkholy, R.A. El-Mallawany, A.c. conductivity of tellurite glasses, Mater. Chem. Phys. 40 (3) (1995) 163–167.
[5] N.S. Hussain, G. Hungerford, R. El-Mallawany, M.J.M. Gomes, M.A. Lopes, N. Ali, J.D. Santos, S. Buddhudu, Absorption and emission analysis of RE^{3+} (Sm^{3+} and Dy^{3+}): lithium boro tellurite glasses, J. Nanosci. Nanotechnol. 9 (2009) 3672–3677.
[6] I.Z. Hagar, R. El-Mallawany, M. Poulain, Infrared and Raman spectra of new molybdenum and tungsten oxyfluoride glasses, J. Mater. Sci. 34 (21) (1999) 5163–5168.
[7] R.A. El-Mallawany, L.M. Sharaf El-Deen, M.M. Elkholy, Dielectric properties and polarizability of molybdenum tellurite glasses, J. Mater. Sci. 31 (23) (1996) 6339–6343.
[8] A. Kaur, A. Khanna, F. Gonzalez, C. Pesquera, B. Chen, Structural, optical, dielectric and thermal properties of molybdenum tellurite and borotellurite glasses, J. Non-Cryst. Solids 444 (2016) 1–10.
[9] M. Anand Pandarinath, G. Upender, K. Narasimha Rao, D. Suresh Babu, Thermal, optical and spectroscopic studies of boro-tellurite glass system containing ZnO, J. Non-Cryst. Solids 433 (2016) 60–67.
[10] M. Ami Hazlin, M. Halimah, F. Muhammad, M. Faznny, Optical properties of zinc borotellurite glass doped with trivalent dysprosium ion, Phys. B Condens. Matter 510 (2017) 38–42.
[11] M.N. Azlan, M.K. Halimah, S.Z. Shafinas, W.M. Daud, Effect of erbium nanoparticles on optical properties of zinc borotellurite glass system, J. Nanomater. (2013) 168.
[12] M.K. Halimah, M.F. Faznny, M.N. Azlan, H.A.A. Sidek, Optical basicity and electronic polarizability of zinc borotellurite glass doped La 3+ ions, Results in Physics 7 (2017) 581–589.
[13] Vincenzo M. Sglavo, Diego Pugliese, Francesco Sartori, Nadia G. Boetti, Edoardo Ceci Ginistrelli, Giuseppe Franco, Daniel Milanese, Mechanical properties of resorbable calcium-phosphate glass optical fiber and capillaries, J. Alloy. Comp. 778 (2019) 410–417.
[14] M.N. Azlan, M.K. Halimah, Role of Nd3+ nanoparticles on enhanced optical efficiency in borotellurite glass for optical fiber, Results in Physics 11 (2018) 58–64.
[15] J.V. Bell, V. Anjos, L.M. Moreira, R.F. Falci, L.R.P. Kassab, D.S. Silva, J.L. Doualan, P. Camy, R. Moncorgé, Laser emission of Nd-doped mixed tellurite and zinc oxide glass, J. Opt. Soc. Am. B 31 (2014) 1590–1594.
[16] T. Wei, Y. Tian, C. Tian, X. Jing, M. Cai, J. Zhang, L. Zhang, S. Xu, Comprehensive evaluation of the structural , absorption , energy transfer , luminescent properties and near-infrared applications of the neodymium doped germanate glass, J. Alloy. Comp. 618 (2015) 95–101.
[17] Hoang Tuan Tong, Daisuke Demichi, Kenshiro Nagasaka, Takenobu Suzuki, Yasutake Ohishi, Suppressing 1.06-μm spontaneous emission of neodymium ions using a novel tellurite all-solid photonic bandgap fiber, Optic Commun. 415 (2018) 87–92.
[18] S.N. Nazrin, M.K. Halimah, F.D. Muhammad, J.S. Yip, L. Hasnimulyati, M. F. Faznny, M.A. Hazlin, I. Zaitizila, The effect of erbium oxide in physical and structural properties of zinc tellurite glass system, J. Non-Cryst. Solids 490 (2018) 35–43.
[19] C. Eevon, M.K. Halimah, A. Zakaria, C.A.C. Azurahanim, M.N. Azlan, M.F. Faznny, Linear and nonlinear optical properties of Gd3+ doped zinc borotellurite glasses for all-optical switching applications, Results in Physics 6 (2016) 761–766.
[20] S. Suresh, P. Gayathri Pavani, V. Chandra Mouli, ESR, optical absorption, IR and Raman studies of xTeO2+(70−x)B2O3+5TiO2+24R2O:1CuO (x=10, 35 and 60mol%; R=Li, Na and K) quaternary glass system", Mater. Res. Bull. 47 (3) (2012) 724–731.
[21] V.E. Derr, Estimation of the extinction coefficient of clouds from multiwavelength lidar backscatter measurements, Appl. Opt. 19 (14) (1980) 2310–2314.
[22] P. Bavafa, M. Rezvani, Effect of Sn doping in optical properties of Se-Ge glass and glass-ceramics, Results in Physics 10 (2018) 777–783.
[23] M.R. Sahar, Ariffin Ramli, Syaridatul Akmar Roslan, Thermal Parameters Er^{3+}/Nd^{3+} Co-doped Tellurite Glass, UMTAS, 2011.
[24] J. Tauc, Optical properties of amorphous semiconductors, in: Amorphous and Liquid Semiconductors, 1974, pp. 159–220.
[25] M.K. Halimah, C. Eevon, Comprehensive study on the effect of Gd2O3 NPs on elastic properties of zinc borotellurite glass system using non-destructive ultrasonic technique, J. Non-Cryst. Solids 511 (2019) 10–18.
[26] V. Dimitrov, T. Komatsu, An interpretation of optical properties of oxides and oxides glasses in term of electronic polarizability and average single bond strength, J. Univ. Chem. Technol. Metal. 45 (2010) 219–250.
[27] M.K. Halimah, A. Azuraida, M. Ishak, L. Hasnimulyati, Influence of bismuth oxide on gamma radiation shielding properties of boro-tellurite glass, J. Non-Cryst. Solids 512 (2019) 140–147.
[28] Vesselin Dimitrov, Takayuki Komatsu, Classification of oxide glasses: a polarizability approach, J. Solid State Chem. 178 (3) (2005) 831–846.
[29] J.A. Duffy, M.D. Ingram, Establishment of an optical scale for Lewis basicity in inorganic oxyacids, molten salts, and glasses, J. Am. Chem. Soc. 93 (1971) 6448.
[30] J.A. Duffy, Optical basicity of titanium (IV) oxide and zirconium (IV) oxide, J. Am. Ceram. Soc. 72 (1989) 10.
[31] H.A.A. Sidek, S.P. Chow, Z.A. Talib, S.A. Halim, Formation and elastic behaviour of lead-magnesium chlorophosphate glasses, Turk. J. Phys. 35 (2004) 65–71.
[32] J. Sun, Q. Nie, X. Wang, S. Dai, T. Xu, G. Wang, Glass formation and properties of Ge–Te–BiI3 far infrared transmitting chalcohalide glasses, Spectrochim. Acta Mol. Biomol. Spectrosc. 79 (2011) 904–908.
[33] S. Iranizad, Z. Dehghani, M. Nadafan, Nonlinear optical properties of nematic liquid crystal doped with different compositional percentage of synthesis of Fe3O4 nanoparticles, J. Mol. Liq. 190 (2014) 6–9.
[34] M.S. Mojdehi, W.M.M. Yunus, K.S. Fhan, Z.A. Talib, N. Tamchek, Nonlinear optical characterization of phosphate glasses based on ZnO using the Z-scan technique, Chin. Phys. B 22 (11) (2013) 117802.
[35] Nie Q. Chen, T. Xu, S. Dai, X. Wang, X. Shen, A study of nonlinear optical properties in Bi_2O_3-WO_3-TeO_2 glasses, J. Non-Cryst. Solids 354 (29) (2008) 3468–3472.
[36] Shanmugavelu, V. Venkatramu, V.V.R. Kanth, Optical properties of Nd^{3+} doped bismuth zinc borate glasses, Spectrochim. Acta Mol. Biomol. Spectrosc. 122 (2014) 422–427.
[37] Tintu, V.P.N. Nampoori, P. Radhakrishnan, S. Thomas, Nonlinear optical studies on nanocolloidal Ga-Sb-Ge-Se chalcogenide glass, J. Appl. Phys. 108 (7) (2010) 1–6.
[38] M.N. Azlan, M.K. Halimah, H.A.A. Sidek, Linear and nonlinear optical properties of erbium doped zinc borotellurite glass system, J. Lumin. 181 (2017) (2017) 400–406.